pubs.acs.org/Biomac

Article

Polyester Dendrimers Based on Bis-MPA for Doxorubicin Delivery

Mara Gonçalves, Visvaldas Kairys, João Rodrigues, and Helena Tomás*

Cite This: *Biomacromolecules* 2022, 23, 20−33

Read Online

ACCESS | Metrics & More | Article Recommendations | Supporting Information

ABSTRACT: Although doxorubicin (DOX) is one of the most used chemotherapeutic drugs due to its efficacy against a wide group of cancer types, it presents severe side effects. As such, intensive research is being carried out to find new nanoscale systems that can help to overcome this problem. Polyester dendrimers based on the monomer 2,2-bis-(hydroxymethyl)propionic acid (bis-MPA) are very promising systems for biomedical applications due to their biodegradability properties. In this study, bis-MPA-based dendrimers were, for the first time, evaluated as DOX delivery vehicles. Generations 4 and 5 of bis-MPA-based dendrimers with hydroxyl groups at the surface were used (B-G4-OH and B-G5-OH), together with dendrimers partially functionalized with amine groups (B-G4-NH_2/OH and B-G5-NH_2/OH). Partial functionalization was chosen because the main purpose was to compare the effect of different functional groups on dendrimers' drug delivery behavior without compromising cell viability, which is often affected by dendrimers' cationic charge. Results revealed that bis-MPA-based dendrimers were cytocompatible, independently of the chemical groups that were present at their surface. The B-G4-NH_2/OH and B-G5-NH_2/OH dendrimers were able to retain a higher number of DOX molecules, but the in vitro release of the drug was faster. On the contrary, the hydroxyl-terminated dendrimers exhibited a lower loading capacity but were able to deliver the drug in a more sustained manner. These results were in accordance with the cytotoxicity studies performed in several models of cancer cell lines and human mesenchymal stem cells. Overall, the results confirmed that it is possible to tune the drug delivery properties of bis-MPA-based dendrimers by modifying surface functionalization. Moreover, molecular modeling studies provided insights into the nature of the interactions established between the drug and the bis-MPA-based dendrimers—DOX molecules attach to their surface rather than being physically encapsulated.

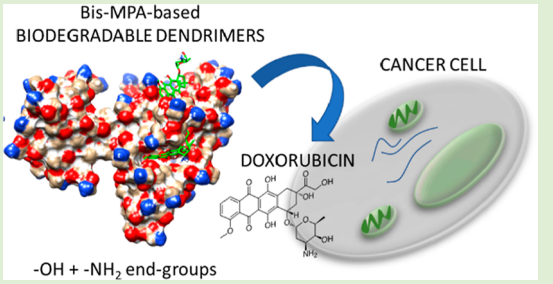

INTRODUCTION

Nanomedicine has the purpose of helping the healthcare system in the diagnosis, treatment, and follow-up of diseases, as well as other medical conditions. Because cancer is an increasing problem worldwide, there is big interest in applying nanomedicine solutions to minimize it, and, in fact, most of the nanomaterials that are being developed envisage applications in this field.[1,2]

Nanomaterials can be made of different materials and shapes.[1] At the moment, polymers are the most studied materials for nanomedicine purposes.[3] They gathered scientists' attention due to the easiness in tuning their properties, such as chemical composition, morphology, size, and biodegradability.[1] Despite this, classical polymers possess a big disadvantage, which is the difficulty in controlling their molecular size with accuracy, a requirement needed for nanomaterials aimed at moving from the bench to the bedside. This difficulty does not apply, however, to all polymer's classes. In fact, among these classes, dendrimers stand out due to their unique architecture and properties. Dendrimers are monodispersed molecules with structural perfection. They are branched molecules that can grow from a central core toward the periphery. With each repeating branching cycle, the dendrimer generation increases, together with its molecular weight and number of peripheral terminal groups. Indeed, this last aspect is responsible for dendrimers' multivalency, another important feature of these molecules. In the biomedical field, dendrimers are regarded as interesting platforms for drug delivery because they can transport small drugs inside their structural voids (encapsulation), by adsorption or by covalent conjugation to their terminal functionalities.[4,5]

The poly(amidoamine) (PAMAM) dendrimers, introduced by Tomalia et al.,[6] are the most studied type of dendrimers, also for drug delivery, probably due to their early commercial availability. Several works have shown that PAMAM dendrimers can be loaded with anticancer drugs and serve as vehicles for their delivery inside tumor cells.[7−11] However, PAMAM dendrimers may present toxicity associated with their surface functional groups, namely those that have amine groups at the periphery, because they display a high positive charge at the physiological pH, which increases with the

Received: April 8, 2021
Revised: November 21, 2021
Published: December 6, 2021

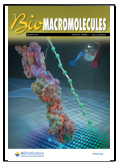

https://doi.org/10.1021/acs.biomac.1c00455
Biomacromolecules 2022, 23, 20−33

Scheme 1. Reaction Scheme for the Surface Modification of the Neutral Generation 4 Bis-MPA Dendrimer (a Fully Functionalized Dendrimer is Shown in the Image)

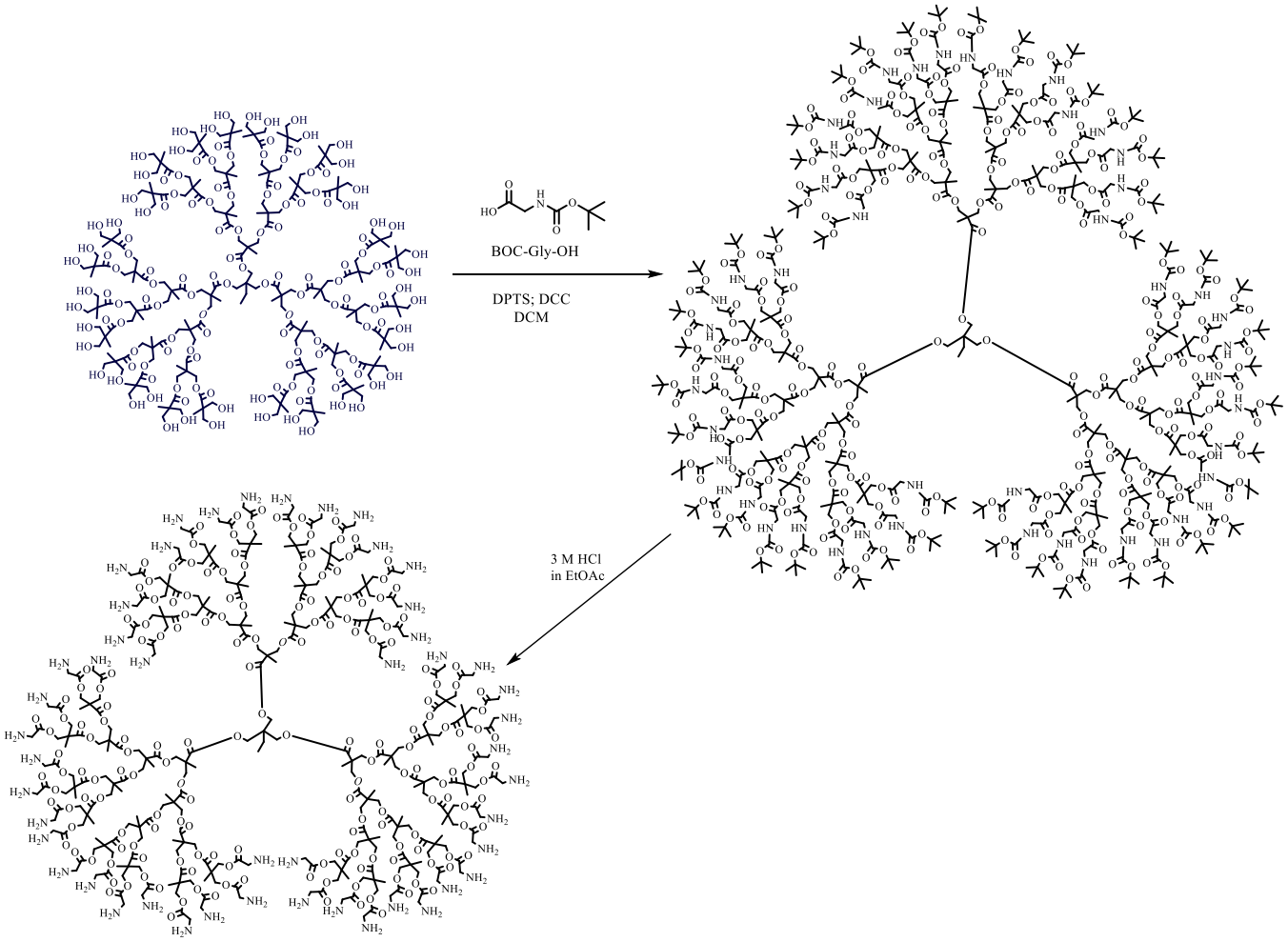

generation number (Gx).[12,13] In order to overcome this issue, a few strategies have been employed, such as the acetylation of the amine groups or conjugation with polymers (e.g., polyethylene glycol) at the surface.[14−18]

One class of dendrimers that are not so extensively explored for drug delivery is the 2,2-bis(hydroxymethyl)propionic acid (bis-MPA)-based polyester family.[19] These dendrimers are biodegradable and, nowadays, also commercially available with different surface functional groups and generations.[20,21] In fact, the existing studies on the use of bis-MPA-based dendrimers for drug and/or gene delivery[22−26] show that they can be an excellent choice as delivery vehicles because they exhibit very good biocompatibility in vitro and in vivo, a high water solubility, and easy surface functionalization. The non-cytotoxic behavior of these systems was also confirmed by Feliu et al. using a library of bis-MPA-based dendrimers with hydroxyl and carboxyl surface groups.[27] More recently, bis-MPA-based dendrimers functionalized with amines were prepared and assayed as siRNA delivery vehicles and antibacterial drugs with promising results.[28,29]

Doxorubicin (DOX) is considered to be one of the first-line treatments in chemotherapy, being used for a variety of cancer types. However, although DOX exhibits a broad spectrum of activity, it also has associated severe side effects, namely cumulative cardiotoxicity and myelosuppression.[30,31] As such, the need to overcome this concern is of major importance and, in this sense, researchers all over the world are trying to develop new nanoscale systems suitable for DOX delivery that will help diminish its secondary effects, as well as improve its biodistribution and efficacy. Although there are already a few DOX-based nanotherapeutics in the market (liposomal systems),[32−34] they still present limitations and the need to search for new solutions persists.

This work aims to evaluate the performance of bis-MPA-based dendrimers for the delivery of DOX into cancer cells. Several cell lines were used as cancer cell models—an osteosarcoma cell line (CAL-72), a breast adenocarcinoma cell line (MCF-7), and an ovarian carcinoma cell line (A2780). The cytotoxicity effect of the DOX-loaded dendrimers was also evaluated using human mesenchymal stem cells (hMSCs) as recent shreds of evidence show that they may have a role in tumor development.[35−37] In fact, some reports reveal that hMSCs are recruited to tumor sites, supporting their development—for example, by suppressing the immune response, enhancing angiogenesis, and inhibiting apoptosis and promoting epithelial to mesenchymal transition and thus metastasis formation. The study was focused on generations 4 and 5 of bis-MPA-based dendrimers with hydroxyl terminal groups (B-G4-OH and B-G5-OH), as such and partially functionalized at the surface with amine groups (B-G4-NH_2/OH and B-G5-NH_2/OH). The objective was to compare the effect of different surface functional groups on dendrimers'

https://doi.org/10.1021/acs.biomac.1c00455
Biomacromolecules 2022, 23, 20−33

performance, without increasing too much their cytotoxic behavior, that is, exposing a moderate number of amines at their periphery. Experiments with PAMAM dendrimers were also done for comparison purposes. As far as we know, this is the first work reporting the use of bis-MPA-based dendrimers as scaffolds for DOX loading and delivery.

EXPERIMENTAL SECTION

Reagents and Materials. Generation 4 (G4) and generation 5 (G5) polyester dendrimers based on bis-MPA with hydroxyl surface groups and a trimethylolpropane core (company codes: PFD-G4-TMP-OH and PFD-G5-TMP-OH that correspond to our compounds B-G4-OH and B-G5-OH, respectively) were bought from Polymer Factory (Sweden). G4 PAMAM dendrimers with amine and hydroxyl surface groups (P-G4-NH_2 and P-G4-OH, respectively) were purchased from Dendritech (USA), as well as G5 PAMAM dendrimers (P-G5-NH_2 and P-G5-OH, respectively). All PAMAM dendrimers had an ethylenediamine core. Regenerated cellulose dialysis membranes (molecular weight cutoff, MWCO = 1 kDa) were obtained from Spectrum Labs. DOX hydrochloride salt (DOX·HCl) was acquired from Zibo Ocean International Trade Co, Ltd. *N*,*N*′-dicyclohexylcarbodiimide (DCC, 99%) was bought from Alfa Aesar. 4-(Dimethylamino)pyridine (DMAP) was obtained from Acros Organics. Triethylamine (TEA) was purchased from Merck. *N*-(*tert*-Butoxycarbonyl) glycine (BOC-Gly-OH), *p*-toluenesulfonic acid monohydrate (PTSA), and formaldehyde solution were from Sigma-Aldrich. Hydrochloric acid (HCl, 37%), ethyl acetate (EtOAc, analytical grade 99.98%), tetrahydrofuran (THF, analytical grade 99.99%), dimethylformamide (DMF, HPLC grade, 99.99%), and dichloromethane (DCM, HPLC grade, 99.99%) were bought from Fisher Scientific. The water used for the experiments was HyClone Water (Molecular Biology Grade) obtained from GE Healthcare Life Sciences. Slide-A-Lyzer mini dialysis devices were purchased from Thermo Fisher Scientific.

Synthesis of 1,4-Dimethylpyridinium p-Toluenesulfonate (DPTS). DPTS was synthesized as described in the literature[38,39] by mixing saturated solutions of DMAP and PTSA in THF at a 1:1 equivalent molar ratio. For the first solution, 2.5 g (0.2 mol, 2 M) of DMAP was dissolved in THF, under stirring, at room temperature (RT). For the second solution, 3.9 g (0.2 mol, 2 M) of PTSA was dissolved in THF, under stirring, at RT. These two solutions were mixed under magnetic stirring, at RT, and a white precipitate was immediately formed. This precipitate was filtered, washed with THF, and dried under vacuum. The structure of DPTS was confirmed by ^{1}H NMR (Figure S1 in the Supporting Information).

Surface Modification of B-G4-OH and B-G5-OH Dendrimers. The surface modification of the hydroxyl-terminated polyester dendrimers based on bis-MPA was made generally following the work developed by Movellan et al.[24] (Scheme 1). Briefly, 1 equiv of each dendrimer was dissolved in dry DCM, followed by the addition of 2 equiv of BOC-Gly-OH and 0.4 equiv of DPTS (per hydroxyl surface group), under an argon atmosphere. Due to solubility difficulties, 1.5 mL of DMF was then added and left 1 h 30 at RT, under magnetic stirring, until complete dissolution. Afterward, the reaction flask was cooled to 0 °C and a solution of 1.5 equiv (per hydroxyl surface group) of DCC, in dry DCM, was added dropwise. The reaction was allowed to proceed for 24 h, at RT, under an argon atmosphere and magnetic stirring. Then, EtOAc was added and the reaction mixture was homogenized. In terms of product recovery, two different procedures were tested. In the case of the B-G4-OH dendrimer, liquid−liquid extraction was used and, later, for the B-G5-OH dendrimer, vacuum filtration was applied (Hirsch-Type Funnel, pore number 4). In the first case, two liquid phases were obtained—on the top was EtOAc with a white precipitate and at the bottom a transparent DCM phase. The transparent DCM phase contained the final crude product, which was collected after solvent evaporation and, later, redissolved in methanol. In the second method, the mixture was filtered after EtOAc addition, separating the white precipitate from the crude product. The second procedure was considered more effective to get a product with higher purity. From this stage on, the procedure was the same for both generations of bis-MPA-based dendrimers whenever it was necessary to repeat the synthesis. The crude products, which were dissolved in methanol, were purified by dialysis (MWCO = 1 kDa) against methanol, for 24 h. On the following day, the solvent was evaporated and the BOC-protected dendrimer based on bis-MPA was obtained. For BOC removal, a typical procedure for deprotection of amino groups was used. Briefly, the product was dissolved in a 3 M solution of HCl in EtOAc and left stirring for 30 min at RT. Then, the solvent was evaporated, and the product was characterized by ^{1}H NMR and ^{13}C NMR.

Characterization of the B-G4-NH_2/OH and B-G5-NH_2/OH Dendrimers. The ^{1}H NMR spectra were acquired on Bruker Avance II+ 400 MHz equipment and used to confirm the surface modification of bis-MPA dendrimers. All the compounds were dissolved in deuterium oxide (D_2O 99.99 atom % D, Sigma-Aldrich) before measurements. Residual ^{1}H resonance from the deuterated solvent was used as reference in the spectra. The ^{13}C NMR spectra were also recorded for the samples using the same solvent and equipment.

Doxorubicin Loading. DOX·HCl was loaded into bis-MPA-based dendrimers (B-G4-OH and B-G4-NH_2/OH; B-G5-OH and B-G5-NH_2/OH) and PAMAM dendrimers (P-G4-OH and P-G4-NH_2; P-G5-OH and P-G5-NH_2) having different generations and end groups. First, dendrimers were dissolved in distilled water. After that, a stock solution of DOX·HCl (4 mg mL^{-1}) was prepared in methanol and then neutralized with TEA (the molar ratio TEA/DOX was 3.33:1). Afterward, the neutralized DOX was added dropwise to the dendrimer solution under magnetic stirring and protected from light. A DOX/dendrimer molar ratio of 5:1 was used. The process proceeded for 4 days, at RT, with the lid slightly opened to allow solvent evaporation. Later on, the mixture was centrifuged at 15,000 rpm for 5 min, and the free DOX precipitate was washed with distilled water three times. The supernatant containing the DOX-loaded dendrimers was collected and lyophilized, and the free DOX precipitate was dissolved in methanol and analyzed by UV−Vis spectroscopy. To calculate the loading efficiency (LE) and loading capacity (LC), a calibration curve of DOX in methanol was prepared using standards of the known concentration. Loading efficiency (%) and loading capacity (%) were calculated according to eqs 1 and 2, respectively.

$$\text{L. E. (\%)} = \frac{\text{mass of loaded DOX}}{\text{initial mass of DOX}} \times 100 \quad (1)$$

$$\text{L. C. (\%)} = \frac{\text{mass of loaded DOX}}{\text{mass of DOX loaded dendrimers}} \times 100 \quad (2)$$

In Vitro Drug Release Studies. The release profile of DOX from bis-MPA-based and PAMAM dendrimers was assessed in vitro using the dialysis cassette system (Slide-A-Lyzer mini dialysis system, MWCO = 2 kDa). Briefly, stock solutions of DOX and DOX-loaded dendrimers were prepared in water at a final concentration of 0.5 mg mL^{-1}. Inside of the dialysis system, a total volume of 0.3 mL was placed, which corresponded to 0.1 mL of dendrimer aqueous solution and 0.2 mL of supplemented cell culture medium, that is, DMEM medium (Sigma-Aldrich) containing 10% (v/v) fetal bovine serum (FBS, Gibco) and 1% (v/v) antibiotic−antimycotic (AA, 100× solution, Gibco). The dialysis system was submerged in 10 mL of supplemented media and incubated at 37 °C. All samples were prepared considering equivalent amounts of DOX (2.5 μg mL^{-1}). At predetermined time points, an aliquot of 0.1 mL of media was withdrawn and substituted by an equal amount of a fresh medium. Experiments in Dulbecco's phosphate-buffered saline solution (DPBS) at different pH values were also performed following a similar methodology. The DOX concentration was determined by fluorimetry using a microplate reader (model Victor^3 1420, PerkinElmer) and a standard calibration curve. The cumulative release (C_r) of DOX over time was calculated according to eq 3,[40] where V_o is the volume of release media, C_n is the measured concentration of DOX in a certain time point, and m_{DOX} is the initial mass of DOX inside of the dialysis system; V_t is the volume of the

https://doi.org/10.1021/acs.biomac.1c00455
Biomacromolecules 2022, 23, 20−33

aliquots previously removed and C_i is the corresponding DOX concentrations in those aliquots. Replicates were performed for each experiment ($n = 3$) and the average was determined.

$$C_r(\%) = \frac{V_o C_n + V_t \times \sum_1^{n-1} C_i}{m_{DOX}} \times 100 \quad (3)$$

Molecular Modeling. The starting geometries for most of the dendrimers, except for PAMAM-NH_2, were generated from the 2D structural formulas using a combination of several tools: MarvinSketch (v. 14.12.1.0) (ChemAxon Ltd), UCSF Chimera (v. 1.11),[41] and Avogadro (v. 1.2.0)[42] The initial rough optimization of the constructed molecules was done using the MMFF94s force field[43] in Avogadro. The starting PAMAM-NH_2 structures were taken from Maiti et al.[44] The amino groups that terminate the dendrimers were fully protonated. The structures of partially aminated bis-MPA dendrimers were generated from fully aminated bis-MPA ones by removing the extraneous amino group-containing tails by hand. Afterward, the structures of the dendrimers were optimized using 50 ns molecular dynamics (MD) simulations in water using a protocol described below. The structure of DOX was taken from Protein Data Bank entry 1p20,[45] and the structures of methanol and TEA were generated using Avogadro. The simulation box was set to cubic with the dendrimer in the center, with a 10 Å distance from the surface of the box to the nearest atom of the dendrimer. Five protonated DOX molecules were added to the simulation box, to simulate the experimental dendrimer-to-DOX ratio. The simulation boxes were also filled with 17 TEA ions, TIP4P waters,[46] methanol, and additional Cl^- or Na^+ ions if necessary to make the system neutral. Two simulations were set up: one with a water solvent only, and another one with a water/methanol mixed solvent, with a 1.5:1 molar ratio close to the experimental conditions. When optimizing a single dendrimer to generate starting structures for the production simulations, only waters and Cl^- ions were added to the simulation box. MD simulations were carried out using the GROMACS (v. 2016.3)[47] program. The OPLS-AA force field[48] was used for the MD simulations. The OPLS-AA parameters for DOX, dendrimers, and other organic species in the solution were generated using the TPPMKTOP web server (http://erg.biophys.msu.ru/tpp/). The generated simulation box was first subjected to the steepest descent minimization until the maximum force on any of the atoms decreased to 1000 kJ·mol^{-1} nm^{-1}. Afterward, a 100 ps equilibration was performed with 2 fs time steps using velocity-rescale temperature coupling and Berendsen pressure coupling. The Particle Mesh Ewald (PME) algorithm was used for electrostatic interactions with a 10 Å cutoff. The same cut-off value was used for van der Waals interactions. The length of the production simulation was set to 200 ns, with similar settings to that for the equilibration, except for the pressure coupling, which used the Parrinello−Rahman algorithm. The snapshots of the MD simulations were taken every 1 ns and the results were analyzed using GROMACS tools and custom scripts. The number of DOX molecules attached to a dendrimer using a 3.5 Å distance cutoff was counted using a custom script, and this also included detection of DOX oligomers bound to the host molecule. For the neighbor count, the statistics was taken from the 10−200 ns interval of the production run, to give time for DOX molecules to diffuse from the bulk to the dendrimer surface.

Cell Culture and In Vitro Cell Viability Assays. Several cell lines were used as cancer cell models—an osteosarcoma cell line (CAL-72, DSMZ, Germany), a breast adenocarcinoma cell line (MCF-7, DSMZ, Germany), and an ovarian carcinoma cell line (A2780, European Collection of Cell Cultures, UK). The cytotoxicity effect of the DOX-loaded dendrimers was also evaluated using hMSCs harvested from small pieces of human trabecular bone from healthy adults obtained during surgical interventions after trauma (only bone that would have been discarded was used, with the approval of the ethics committee from Funchal Central Hospital). CAL-72 cells were cultured in DMEM medium containing 10% (v/v) fetal bovine serum FBS (Gibco), 1% (v/v) insulin−transferrin−sodium selenite (100× solution, Gibco), 2 mM L-glutamine (Gibco), and 1% (v/v) AA solution. MCF-7 cells were grown in RPMI 1640 medium (Sigma-Aldrich) supplemented with 10% (v/v) FBS, 1% (v/v) non-essential amino acids (NEAA, 100× solution, Gibco), 1 mM sodium pyruvate (Sigma-Aldrich), 0.3 μg mL^{-1} human insulin (Gibco), and 1% (v/v) AA solution. A2780 cells were cultured in RPMI 1640 medium supplemented with 10% (v/v) FBS, 2 mM L-glutamine, and 1% (v/v) AA solution. The hMSCs were grown in α-MEM medium (Sigma-Aldrich) supplemented with 10% (v/v) FBS and 1% (v/v) AA solution. For the experiments, cells were cultured at 37 °C, in a humidified atmosphere with 5% (v/v) carbon dioxide (CO_2), being harvested when 70—80% of confluency was reached. The cells were then seeded in 24-well plates at a cell density of 10,000 cells per well. One day after, aqueous solutions of free DOX, DOX-loaded bis-MPA-based dendrimers/PAMAM dendrimers (with equivalent DOX concentrations), and, also, non-loaded dendrimers (used as controls with equivalent dendrimer mass concentrations) were prepared. The cells were further incubated with these systems for 48 h. Cell viability was indirectly measured through the resazurin reduction assay, which relies on the metabolic activity of cells. Briefly, after 48 h of incubation time, the cell medium was removed and replenished with a fresh medium containing resazurin (Sigma-Aldrich) with a final concentration of 0.1 mg mL^{-1}. Afterward, the cells were kept in the incubator for 3 h. In the end, aliquots of the media were transferred to an opaque 96-well plate and resorufin fluorescence was measured in the microplate reader (model Victor3 1420, Perkin Elmer). The results are presented as a percentage of the metabolic activity relative to the control and corresponding to the mean of three replicates.

Cells were observed using a fluorescence microscope after 48 h in contact with the test solutions. For this, cells were washed with sterilized DPBS solution and fixed with 3.7% formaldehyde (Sigma-Aldrich). After removing the fixative solution, the cell nucleus was stained using 4′,6-diamidino-2-phenylindole dilactate (DAPI, Sigma-Aldrich) for 30 min. To conclude the process, the cells were washed two times with DPBS solution and finally washed with ultrapure water (Milli-Q system, Millipore). Pictures were taken using an optical fluorescence microscope (Nikon Eclipse TE 2000E inverted microscope).

Statistics. Statistical analyses were performed using the GraphPad Prism 7. One-way ANOVA with Tukey Post Hoc test was used to assess the statistical difference between free drug and DOX-loaded dendrimer group means. A probability level of $p < 0.05$ was considered to be significant.

RESULTS AND DISCUSSION

This study aimed at the investigation of bis-MPA-based dendrimers as vehicles for DOX delivery. Generations 4 and 5 of bis-MPA-based dendrimers with hydroxyl groups at the surface (B-G4-OH and B-G5-OH) were tested, as well as dendrimers partially functionalized with amine groups (B-G4-NH_2/OH and B-G5-NH_2/OH). As such, starting from bis-MPA dendrimers with hydroxyl end groups, bis-MPA dendrimers partially functionalized with amine termini were first prepared and characterized using suitable physicochemical techniques. Then, all hydroxyl-terminated and hydroxyl/amine-terminated dendrimers based on bis-MPA were loaded with DOX and their in vitro drug release profile as well as their cytotoxic behavior were studied. Molecular modeling studies were further performed to understand how the dendrimers interact with DOX molecules. For comparative purposes, the experiments were also done with PAMAM dendrimers. All results are presented and discussed in more detail in the following sections.

Preparation and Characterization of Amine Partially Functionalized B-G4-NH_2/OH and B-G5-NH_2/OH Dendrimers. Generation 4 and generation 5 bis-MPA dendrimers with hydroxyl surface groups were modified to obtain dendrimers with amine termini through a two-step reaction.

https://doi.org/10.1021/acs.biomac.1c00455
Biomacromolecules 2022, 23, 20−33

In the first stage, the dendrimers were conjugated to BOC-Gly-OH and afterward deprotected under acidic conditions. The partially modified bis-MPA dendrimers with amine termini were characterized by ^{1}H NMR and ^{13}C NMR using D_2O as solvent (spectra are shown in the Supporting Information). In the ^{1}H NMR spectra, the solvent signal was identified at δ = 4.79 ppm (reference) and multiple signals were attributed to bis-MPA-based dendrimer protons. Signal integration was made considering the characteristic proton signals from the $-CH_2O-$ group ($\delta \approx 4.40$ to 4.22) that corresponds to 90 protons (in generation 4) or 186 protons (in generation 5) for the bis-MPA-based dendrimers with hydroxyl termini and the bis-MPA-based dendrimers partially functionalized with amines, respectively. For both dendrimer generations, the successful surface modification with amine groups is represented by the appearance of a new proton signal at $\delta \approx$ 4.0 ppm ($-CH_2NH_2$).

In accordance with the ^{1}H NMR spectra, the surface modification of the dendrimers was not fully complete, that is, only a partial modification of the hydroxylated bis-MPa-based dendrimers was obtained, which was the initial objective. Indeed, whereas the full surface modification of the B-G4-OH dendrimer would result in a total of 48 amine surface groups, only a total of 17 amine termini were achieved corresponding to 35% of surface modification (Figure S4 in the Supporting Information). For the B-G5-OH dendrimer, a complete modification would correspond to a total of 96 amine surface groups and, in this case, only 42 amine termini were detected, which corresponds to 44% of surface modification (Figure S6 in the Supporting Information). As expected, these are mean values because the functionalization was statistical. The ^{13}C NMR spectra reveal the expected characteristic signals of the prepared compounds (Figures S5 and S7 in the Supporting Information).

Drug Loading. Both bis-MPA-based dendrimers and PAMAM dendrimers were loaded with DOX. Essentially, a solution of DOX was prepared in methanol and added dropwise to the dendrimer aqueous solution. Although the DOX-loaded dendrimers remained in solution, the free DOX (non-loaded drug) formed a precipitate, which was later dissolved in methanol for DOX quantification. UV−Vis spectrophotometry was then used for the indirect determination of the amount of DOX retained in the dendrimers. The results regarding the loading efficiency (LE) and the loading capacity (LC) are present in Table 1 for all dendrimer types. LE corresponds to the percentage (w/w) of drug used in the loading process that was retained inside dendrimers. LC corresponds to the percentage (w/w) of DOX in the loaded dendrimer.

Table 1. LE and LC for PAMAM and Bis-MPA-Based Dendrimers (Both Generations 4 and 5)

sample	LE (% w/w)	LC (% w/w)
P-G4-OH/DOX	61 ± 1	13 ± 1
P-G4-NH_2/DOX	42 ± 1	8 ± 1
B-G4-OH/DOX	37 ± 2	17 ± 1
B-G4-NH_2/OH/DOX	100 ± 1	26 ± 1
P-G5-OH/DOX	42 ± 5	9 ± 1
P-G5-NH_2/DOX	75 ± 1	7 ± 1
B-G5-OH/DOX	33 ± 5	8 ± 1
B-G5-NH_2/OH/DOX	100 ± 1	12 ± 1

As shown in Table 1, the LC values were 17, 8, 26, and 12% for B-G4-OH, B-G5-OH, B-G4-NH_2/OH, and B-G5-NH_2/OH, respectively. As such, the LC increased for bis-MPA-based dendrimers after partial functionalization with amine groups at the surface. Interestingly, the lower generation dendrimers (B-G4-OH and B-G4-NH_2/OH) achieved superior LC values than the higher generations (B-G5-OH and B-G5-NH_2/OH). Loading efficiencies were about 100% for bis-MPA-based dendrimers after partial functionalization with amine groups at the surface, meaning that practically all the initial mass of DOX was loaded to these dendrimers. A DOX/dendrimer ratio of 5:1 was used in the loading process, this means that each dendrimer was able to carry five molecules of DOX. Probably, increasing this ratio would result in a higher number of DOX molecules per dendrimer.

When comparing the LC of bis-MPA-based dendrimers and PAMAM dendrimers, it can be observed that, for the same generation, the amine-terminated bis-MPA-based dendrimers exhibit higher cargos, especially for generation 4 dendrimers. From all the studied dendrimers, the B-G4-NH_2/OH dendrimer was the one that achieved a higher LC (26%). It should be noticed that bis-MPA-based dendrimers have lower molecular weights and a lower number of surface functional groups than PAMAM dendrimers (48 and 96 surface groups for generations 4 and 5 in bis-MPA-based dendrimers, respectively, vs 64 and 128 for PAMAM dendrimers) and that, in addition, bis-MPA-based dendrimers were only partially functionalized with amine groups, whereas the PAMAM dendrimers used in this study were commercially acquired and are fully functionalized. These findings should be advantageous in terms of cytotoxic behavior. Also, bis-MPA-based dendrimers have the additional advantage of being biodegradable.

A panoply of works reported the use of PAMAM dendrimers as potential vehicles for DOX encapsulation.[7,8,10,49−52] However, as previously mentioned and as far as we know, this work is the first to report the use of bis-MPA dendrimers as potential delivery vehicles for DOX. Zeng et al.[22,53] used bis-MPA-based polymers for DOX delivery too but the design of the carrier systems was different. They prepared copolymer micelles were made of poly(ethylene glycol) (PEG)-modified hyperbranched polyester Boltorn H30 and H40 polymers (that are polymers of bis-MPA) for DOX delivery. These micelles were also able to be loaded with DOX molecules presenting a LE ranging from 31 to 43% and a drug/carrier ratio (w/w) ranging from 3.1 to 4.3%.

In Vitro Drug Release. One of the main goals of an ideal drug carrier is to release the encapsulated drug in a sustained manner. The in vitro drug release behavior of B-G4-OH, B-G5-OH, B-G4-NH_2/OH, and B-G5-NH_2/OH dendrimers was studied in cell culture medium (supplemented with 10% FBS and 1% AA), at pH 7.4 and 37 °C (Figure 1). The idea was to use a medium that simulates the fluid in the physiological environment and, simultaneously, that will allow a direct correlation of the obtained results with those of cytotoxicity obtained in in vitro cell culture experiments. For comparative purposes, in vitro DOX release studies were also carried out in parallel with DOX-loaded PAMAM dendrimers.

Figure 1 shows that all the materials presented sustained DOX release profiles, although the release was faster in the first hours of the experiments. B-G5-NH_2/OH/DOX dendrimers had a faster release of drug in the first 4 h (~70%), followed by a slow-release, achieving about 100% of cumulative release

https://doi.org/10.1021/acs.biomac.1c00455
Biomacromolecules 2022, 23, 20−33

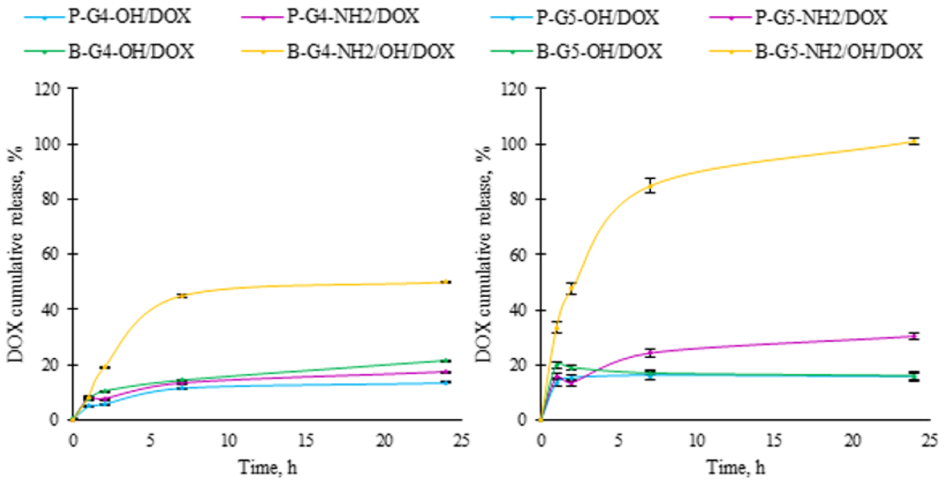

Figure 1. Cumulative release of DOX from bis-MPA-based and PAMAM dendrimers in cell culture media supplemented with 10% FBS and 1% AA (pH 7.4) at 37 °C. Free DOX was dissolved in water and released under the same conditions giving a burst release (not shown). All the samples presented the same DOX content. Data are expressed as a percentage of the total amount of DOX content in the samples, mean ± SD (n = 3).

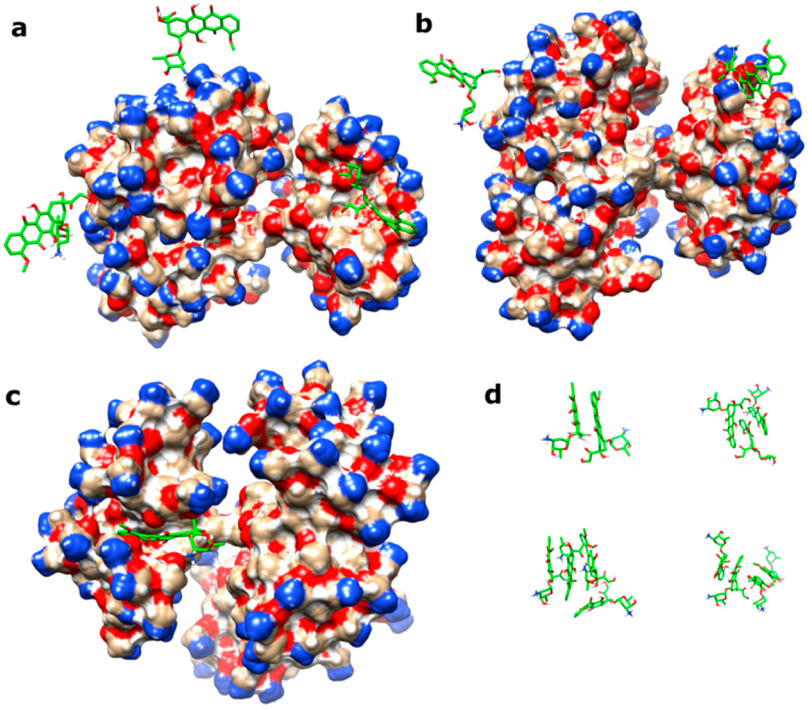

Figure 2. MD simulations of the B-G5-NH_2/DOX system. Snapshots (a) and (b) were taken from the mixed solvent simulation, while (c) from the aqueous solution simulations. Nitrogen atoms are shown in blue, oxygens in red, and DOX molecules are shown in green. Plates (a,b) illustrate type 1 (very weak, DOX molecules on the left side of the dendrimer) and type 2 (intermediate strength, DOX molecules on the right side of the dendrimer) interactions. Plate (b) is a rotation of Plate (a), to better highlight deep clefts inside of the dendrimer. Plate (c) shows DOX molecules deeply inside a cleft, strongly interacting with the dendrimer (type 3). Plate (d) exhibits a typical DOX dimer, trimer (upper row), and two tetramers (lower row).

after 24 h. The B-G4-NH_2/OH/DOX dendrimers presented a more sustained release of DOX as, after a 24 h incubation period, less than 45%, of the drug was released (around 2.2 times less). All the other dendrimers (B-G4-OH, B-G5-OH, and PAMAM dendrimers) presented similar drug release profiles achieving very low DOX cumulative release values after 24 h (between 10 and 25% of cumulative release).

Drug release was followed for a longer period of time in Dulbecco's phosphate-buffered saline (DPBS) solution (7 days), again revealing a sustained release of DOX in all situations (Figure S10 in the Supporting Information). Independently of the pH value, drug release was always faster for the partially functionalized bis-MPA-based dendrimers when compared with the others. At pH of 7.4, until 24 h, the extension of drug release was similar in cell culture medium and DPBS solution for the B-G4-NH2/OH/DOX dendrimers, whereas it was higher in cell culture medium for the B-G5-NH_2/OH/DOX dendrimers. However, the cell culture medium has a much more complex composition than DPBS solution and better reflects what will happen in the cell culture assays, as well as in possible future in vivo applications. Further drug release experiments were performed in DPBS solution to

https://doi.org/10.1021/acs.biomac.1c00455
Biomacromolecules 2022, 23, 20−33

evaluate the effect of pH on the process. A decrease of pH from 7.4 to 5.5 seems to diminish the extent of drug release in all dendrimers at the same time points, being this effect more pronounced for B-G5-NH2/OH/DOX dendrimers. As the pH in the microenvironment of solid tumors can be lower than in healthy tissues due to changes in metabolic processes, this behavior may be beneficial as a more sustained release of DOX from these systems will occur under acidic conditions.

DOX Interaction with Dendrimers. MD simulations were performed to better understand the type of interactions established between DOX molecules and bis-MPA-based dendrimers. For comparison purposes, these studies were also done for bis-MPA dendrimers fully functionalized with amines at the surface (B-G4-NH2 and B-G5-NH2) and for PAMAM dendrimers. The 200 ns MD simulations with one dendrimer and 5 DOX molecules in the simulation box were done both in mixed solvent and in aqueous environments. The former was to mimic experimental conditions used in this work, and the latter was done to compare the results with the results obtained by other groups because aqueous conditions are the most commonly used in the simulations. In addition, a comparison of simulations in different solvent environments can lead to useful insights. For example, mixed solvent MD simulations can be used to probe the binding pockets of hosts due to a different affinity of the solvent components to the surface of the host.[54,55]

To evaluate at a glance the ability of dendrimers to form complexes with DOX, the number of DOX molecules bound to a dendrimer was computed during the simulation and is presented and discussed in more detail in the Supporting Information (Table S1 and the corresponding text). The behavior of the partially functionalized bis-MPA-NH2/OH dendrimers with respect to the number of bounded DOX was essentially intermediate between the fully functionalized bis-MPA-NH2 and bis-MPA-OH dendrimers. Examination of simulation snapshots reveals that binding between the dendrimer and DOX can be roughly classified into three categories: (1) barely touching the surface of the dendrimer, often only binding through a single hydrogen bond (Figure 2a,b), (2) attaching to the shallow pocket lined with the partly hydrophobic core of the dendrimer (Figure 2a,b), and (3) lodging in a pocket-like crevice in the surface of the dendrimer (Figure 2c). The boundary between these categories is not always clearly cut because the process of adsorption of DOX to dendrimer often gradually proceeds through all three stages. For the sake of convenience, we will refer to these binding modes as types 1−3.

Let us first consider the B-G5-NH_2/DOX complex as an example (Figure 2a−c). The distinctive feature of the B-G5-NH_2 dendrimer is that the protonated amino groups at the surface of the dendrimer seem to try to repel each other, which is a probable reason why the dendrimer has a rather extended conformation (Figure 2a−c), assuming a roughly spherical shape. However, the number of the terminal amino groups is far too low to fully cover the surface of the sphere, therefore large chunks of the inner, partly hydrophobic, core of the dendrimer are exposed to the solvent (Figure 2a−c). As a result, the surface of the dendrimer is full of deep crevices of varying width. Examination of the B-G5-NH_2/DOX snapshot data reveals that DOX molecules bind to the dendrimer via the three types of contacts described above: type 1 (weak binding, most often through a single hydrogen bond) (Figure 2a,b), type 2 (sticking or stacking to the hydrophobic surface of the dendrimer) (Figure 2a,b), and type 3 (being caught in a crevice) (Figure 2c). Interestingly, the mixed solvent simulation exhibited mostly the first and the second binding modes. In the aqueous solution simulation, only one DOX molecule was stuck in the crevice during most of the simulation time: only in a single snapshot out of 200, there were contacts with more than one DOX molecule (cf. Table S1). It should be noted that binding of DOX to the dendrimer was always a dynamic process: for example, type 3 contact in Figure 2c started from a type 2 contact at 7 ns (not shown) and gradually the DOX molecule worked its way rather deeply into the dendrimer (Figure 2c). We hypothesize that deep, narrow mostly hydrophobic crevices in mixed solvents apparently have a greater affinity with the methanol compared to DOX and therefore DOX is not able to be drawn inside such a pocket, at least not for long. In water, on the contrary, the hydrophilic environment may be able to push DOX into such a hydrophobic pocket, even in spite of the repulsion of the positive charges on both host and guest molecules.

To further understand the behavior of dendrimer/DOX systems, it is important to note that in our simulations DOX often formed dimers or even occasional trimers/tetramers (the latter seems to most often form by two dimers encountering each other during simulation) (Figure 2d). The formation of dimers was observed experimentally and in other simulations.[56,57] DOX molecules in dimers are usually stacked parallel to each other, likely by $\pi-\pi$ stacking mechanism. The same can be said about the trimer (Figure 2d, above). The tetramer can be best described as a combination of a parallel and perpendicular $\pi-\pi$ stacking (Figure 2d, bottom).[58] It should be noted that experimentally only dimers of DOX but not higher-order aggregates were observed.[59] The discrepancy can probably be explained by a higher concentration of DOX used in the simulation, compared to the experimental conditions. Indeed, DOX tetramers had a more prominent tendency to form in pure aqueous environment simulations compared to the mixed solvent. This is consistent with a much poorer solubility of DOX in water compared to the solvent containing methanol: the hydrophilic environment in water drives hydrophobic DOX rings to bind together. As a consequence, bulky, charged stacked DOX oligomers are much less likely to penetrate the positively charged outer sphere of the B-G5-NH_2 dendrimer and to enter the crevice inside of the dendrimer. In addition, splitting of the DOX monomer off the oligomer will cost much more energy in the hydrophilic aqueous environment compared to the mixed solvent. This might explain why only one DOX monomer was bound to the B-G5-NH_2 dendrimer during most part of the simulations (as shown in Figure 2c). Notably, the formation of stacked oligomers reduces the effective concentration of DOX monomers in the solution that can bind effectively to the dendrimer, which should be a more prominent effect in the aqueous environment.

Because of the absence of the charged groups, the behavior of hydroxyl-terminated dendrimers is expected to be quite different from the dendrimers functionalized with amino groups. Indeed, Table S1 indicates that a relatively large number of DOX molecules in the simulation was bound to the hydroxylated dendrimers. Similar to the amino-functionalized dendrimers, a larger number of DOX molecules are bound in the aqueous solution compared to the mixed solvent. Figure 3 shows typical snapshots from B-G5-OH/DOX simulations. The irregularly shaped dendrimer itself is rather compact and

https://doi.org/10.1021/acs.biomac.1c00455
Biomacromolecules 2022, 23, 20−33

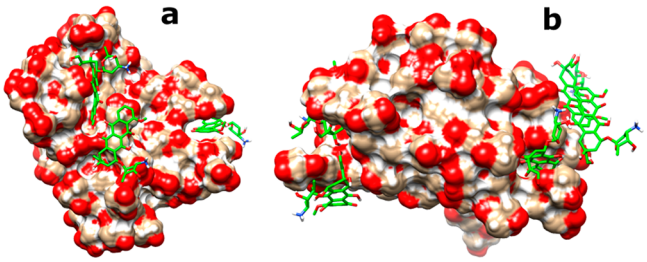

Figure 3. Illustrative snapshots from the B-G5-OH/DOX simulations. Snapshot (a) was taken from the mixed solvent simulation, while (b) from the aqueous solution simulation. Some DOX molecules are wedged in the deep clefts, and several are attached to the surface. The two rightmost DOX molecules in plate (b) form a stacked dimer.

has multiple deep clefts in its surface in both aqueous and mixed solvents. In the mixed solvent simulation snapshot (Figure 3a), three DOX molecules are bound: two belong to "type 3" interactions (bound in deep clefts) and one has a "type 2" interaction (attached to the relatively flat area of the dendrimer surface). In the aqueous solution snapshot portrayed in Figure 3b, all five DOX molecules are bound to the dendrimer, including two DOX in the form of the stacked dimer. Two of the DOX molecules belong to "type 3" interactions, and one DOX monomer and DOX dimer exhibit a "type 2" interaction.

It was interesting to observe if partially functionalized bis-MPA-NH_2 dendrimers behave similar to the bis-MPA-NH_2 and/or bis-MPA-OH dendrimers. Figure 4 contains two

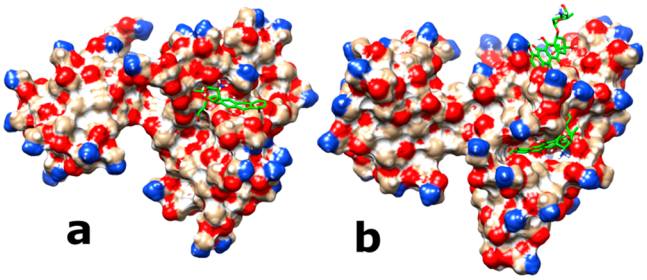

Figure 4. Snapshots from the simulation of the partially functionalized B-G5-NH_2/OH dendrimer. Plate (a) was taken from the mixed solvent simulation, while (b) from the aqueous solution simulation. DOX molecules are either attached to the surface or wedged inside the deep clefts.

snapshots from the simulation of the B-G5-NH_2/OH dendrimer. Compared to the B-G5-NH_2/DOX simulations above described, the partially functionalized dendrimer has fewer charged amino groups that repel DOX charged molecules. Similar to B-G5-OH and B-G5-NH_2 dendrimers, it also presents deep crevices that can accommodate guest molecules. As a result, the behavior of partly functionalized B-G5-NH_2/OH is intermediate between fully aminated and hydroxylated bis-MPA dendrimers.

Simulation results for PAMAM dendrimers are presented in the Supporting Information (Figures S11 and S12). We will not go into deep details regarding the smaller Generation 4 dendrimer simulations because the behavior of these dendrimers should be in many aspects similar to the behavior of the higher generation dendrimers. An interesting exception is the fully functionalized B-G4-NH_2 and the partially functionalized B-G4-NH_2/OH that show a distinct behavior in water: DOX almost do not bind to the fully functionalized B-G4-NH_2 dendrimer (Table S1). Analysis of simulation trajectories (not shown) reveals that this can be best explained by the relative lack of crevices on the surface of the relatively small B-G4-NH_2 dendrimer in combination with its positive charge.

Indeed, to the best of our knowledge, this is the first study describing the interactions between DOX and bis-MPA-based dendrimers. In summary, we found that hydrogen bonding is the most common type of interaction when DOX is bound to a dendrimer. However, the binding was often strengthened by stacking or van der Waals interactions, which mostly take place when DOX enters the cavities and clefts on the surface of the dendrimer. The binding of DOX can be negatively affected by the stacking of two or more DOX molecules together, which reduces the effective concentration of DOX monomers, especially in the aqueous solution.

In Vitro Cytotoxicity Studies. The cytotoxicity of the DOX-loaded bis-MPA-based dendrimers and PAMAM dendrimers was assessed by in vitro cell culture experiments. For that purpose, the cells were exposed to non-loaded and DOX-loaded dendrimers at increasing DOX concentrations (from 0.1 to 5 μM). After 48 h exposure, the viability of cells was evaluated by measuring their metabolic activity using the resazurin reduction assay. The results are shown in Figures 5 and 6, being expressed as a percentage of cell viability in relation to the control, that is, cells that were not exposed to DOX. Different cell lines were used as cancer cell models, namely an osteosarcoma cell line (CAL-72), a breast adenocarcinoma cell line (MCF-7), and an ovarian carcinoma cell line (A2780). The effect of DOX release over hMSCs was also evaluated because, as mentioned before, these cells have been implicated in supporting tumor growth.[35,36]

In general, the non-loaded bis-MPA-based dendrimers were not cytotoxic for all concentrations studied and for all cell types used. Mild cytotoxic effects were only observed for generation 5 bis-MPA-based dendrimers when using CAL-72 cells. This is not surprising because it is known that dendrimer cytotoxicity may depend on the cell type.[12] The PAMAM dendrimers possessing higher amine groups at the surface, due to their strong cationic nature, were especially cytotoxic, being clear that cell viability decreased with increasing dendrimer concentration. One should notice that the cytotoxicity evaluation of non-loaded dendrimers presented in Figures 5 and 6 was made at dendrimer concentrations equivalent to those used in the DOX-loaded dendrimer assays, where the DOX concentration ranged from 0.1 to 5 μM. As bis-MPA-based dendrimers can carry a higher number of DOX molecules, this means that the tested molar concentrations for non-loaded bis-MPA-based dendrimers were lower than those in the case of PAMAM dendrimers. However, like the bis-MPA-based dendrimers, in most experiments, the PAMAM dendrimers with hydroxyl terminal groups were not cytotoxic. These results are in agreement with the information available in the literature, which reveals that PAMAM dendrimers present generation and surface functional group-dependent toxicity.[60−65]

As expected, the toxic effect caused by the free drug increased with its concentration and was also dependent on the cell type. When bis-MPA-based dendrimers were loaded with DOX, the results showed a good correlation with their drug release profiles. In general, in all cell types, the B-G4-NH_2/OH/DOX and the B-G5-NH_2/OH/DOX dendrimers led to

https://doi.org/10.1021/acs.biomac.1c00455
Biomacromolecules 2022, 23, 20−33

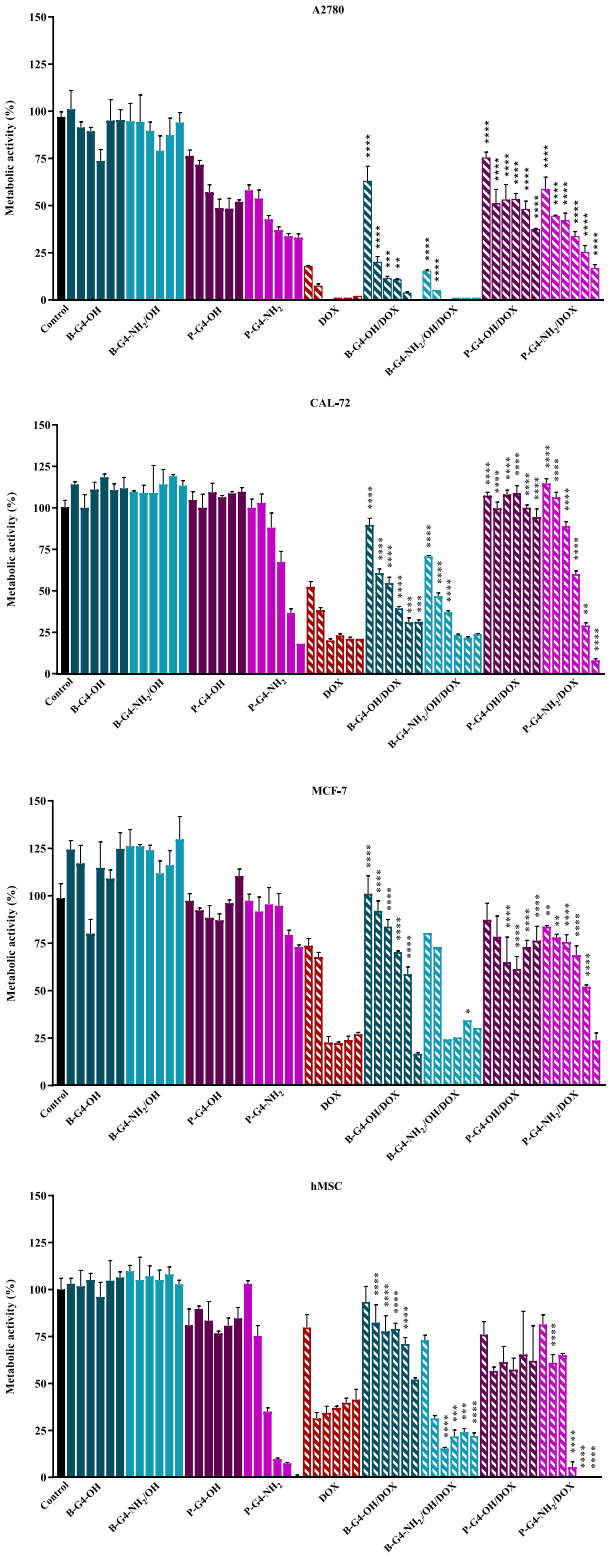

Figure 5. Cell viability of different cancer cell lines (MCF-7, A2780, and CAL-72) and hMSCs after 48 h exposure to the DOX-loaded dendrimers (generation 4, G4) within a range of increasing DOX concentrations (0.1, 0.5, 1, 2, 3, and 5 μM). Free DOX and non-loaded dendrimers were used as controls. Data are expressed by mean ± SD (n = 3). One-way ANOVA with Tukey's Post Hoc test was used to assess the statistical difference between the free DOX mean and the DOX-loaded dendrimer mean (*p < 0.0332, **p < 0.0021, ***p < 0.0002, and ****p < 0.0001).

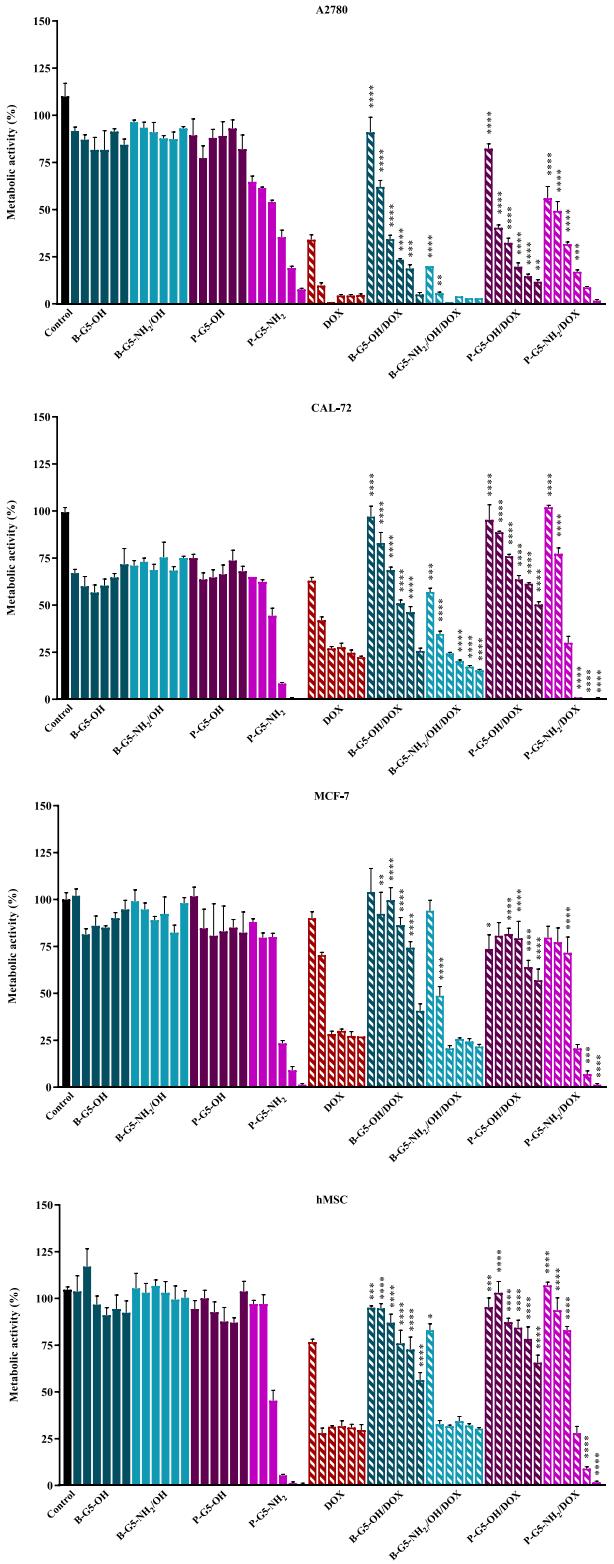

Figure 6. Cell viability of different cancer cell lines (MCF-7, A2780, and CAL-72) and hMSCs after 48 h exposure to the DOX-loaded dendrimers (generation 5, G5) within a range of DOX concentrations (0.1, 0.5, 1, 2, 3, and 5 μM). Free DOX and non-loaded dendrimers were used as controls. Data are expressed by mean ± SD (n = 3). One-way ANOVA with Tukey's Post Hoc test was used to assess the statistical difference between the free DOX mean and DOX-loaded dendrimer mean (*p < 0.0332, **p < 0.0021, ***p < 0.0002, and ****p < 0.0001).

https://doi.org/10.1021/acs.biomac.1c00455
Biomacromolecules 2022, 23, 20−33

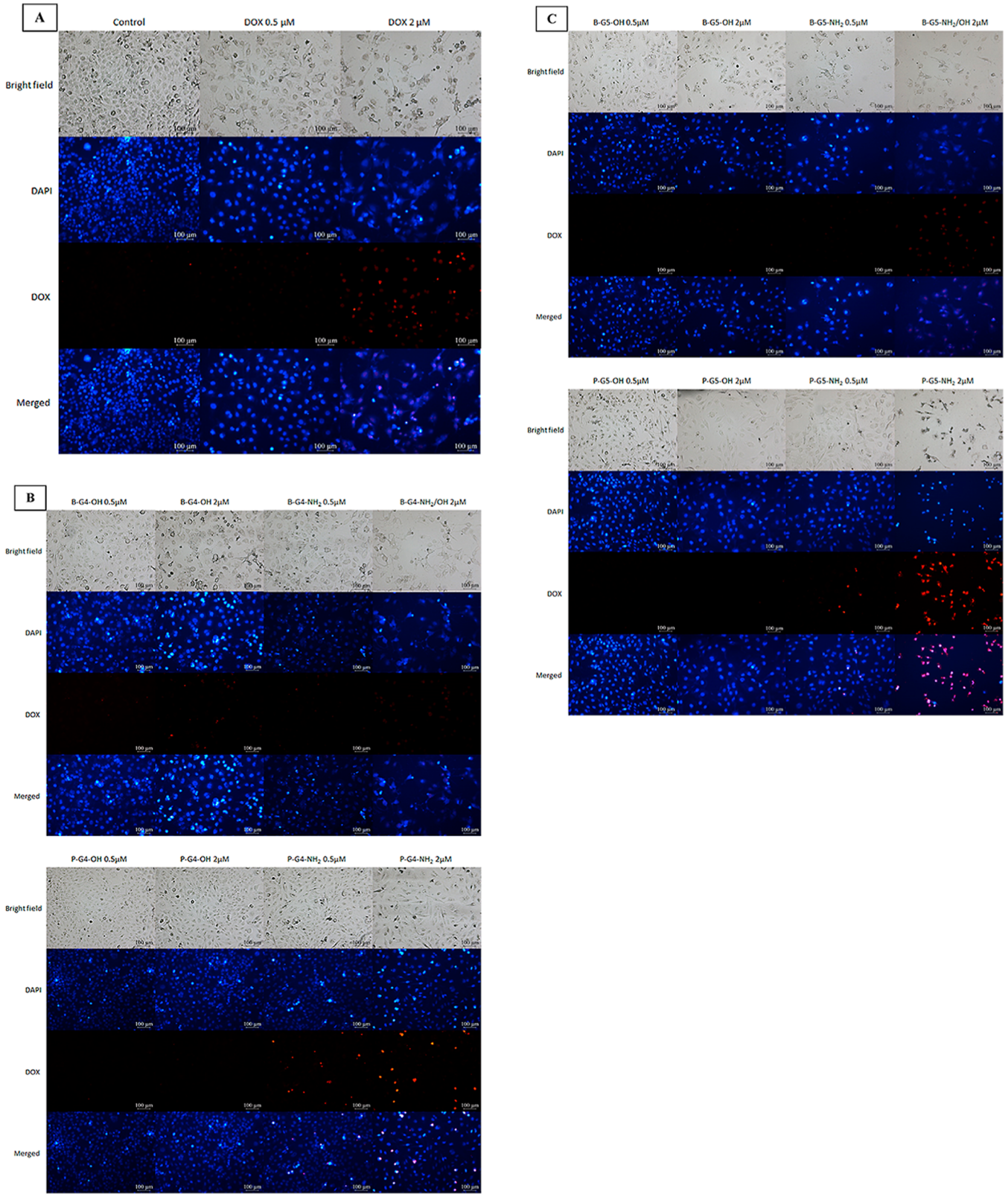

Figure 7. Bright-field and fluorescence microscopy images of CAL-72 cancer cells after 48 h culture with: (A) cells only cultured in cell culture medium and cells cultured in the presence of free DOX (controls); (B) DOX-loaded PAMAM and bis-MPA-based dendrimers (generation 4); and (C) DOX-loaded PAMAM and bis-MPA-based dendrimers (generation 5). The cell nucleus is stained with DAPI (blue fluorescence); DOX gives a red fluorescence signal.

higher cytotoxicity than the B-G4-OH/DOX and the B-G5-OH/DOX dendrimers for which drug was released at a lower rate. Therefore, the bis-MPA-based dendrimers partially functionalized with amine groups at the surface were not intrinsically toxic (due to the reduced number of amine groups) but, when loaded with DOX, led to a level of toxicity

https://doi.org/10.1021/acs.biomac.1c00455
Biomacromolecules 2022, 23, 20−33

equivalent to that caused by the free drug or even higher (see, e.g., the case of the ovarian cancer cell line A2780, which was shown to be particularly sensitive to the DOX presence). Also, for these loaded dendrimers, toxicity increased with the DOX concentration. Likely, these dendrimers act as good drug carriers and facilitate the entrance of DOX inside cells. In a long term and due to its slow drug release profile, one may expect a better therapeutic performance for the B-G4-NH_2/OH/DOX platform when compared with the B-G5-NH_2/OH/DOX one or the use of free DOX. The same applies to the B-G4-OH/DOX and the B-G5-OH/DOX systems for which cytotoxicity is not so pronounced at the beginning but may potentially happen over a longer period of time.

Regarding the PAMAM dendrimers, in general, the cytotoxic behavior of P-G4-OH/DOX and P-G5-OH/DOX was lower than that for all other DOX-loaded dendrimers. On the contrary, the P-G4-NH_2/DOX and the P-G5-NH_2/DOX dendrimers showed dose-dependent cytotoxicity that should also be related to their strong cationic nature, and not only to the drug itself, because the extension of DOX release was limited for these dendrimers (Figure 1).

Although bis-MPA-based dendrimers completely functionalized at the surface with amine groups were not evaluated in the present work, cytotoxicity studies made with bis-MPA-based dendrimers with amino end groups afforded by attachment of boc-protected β-alanines showed that G2 to G4 dendrimers were non-toxic up to 10 μM in several cell lines [rat astrocytes, rat glioma (C6), and human glioblastoma (U87)].[28] When primary neurons were used, however, the G3 and G4 showed dose-dependent toxicity in the range 1−5 μM for G3 and 0.1−1 μM for G4. In our studies with the non-loaded B-G4-NH2/OH and B-G5-NH2/OH partially functionalized dendrimers, concentrations were approximately in the range 1−3 μM and no cytotoxicity was observed for all cell lines studied, with exception for the B-G5-NH2/OH dendrimer in CAL-72 cells. Our results thus confirm that cytotoxicity not only depends on the nanomaterial but also on the type of cells used in the assays.

The antitumor efficacy of the DOX-loaded dendrimers was further validated by fluorescence microscopy. The cell morphology is one of the factors to consider when assessing the effects of drugs, that is, to evaluate if the cells remained healthy or have undergone a death process. Thus, the morphology of the tested cell lines was observed in the microscope after the fixation and staining processes. Figure 7 shows the aspect of the CAL-72 cells after 48 h exposure to DOX-loaded dendrimers (experiments were performed at DOX concentrations of 0.5 and 2 μM). Cells cultured in cell culture medium and in the presence of free DOX were used as controls. When healthy, cells exhibit a fusiform shape and are adherent to the bottom of the cell culture plate. Our results show that these features were preserved in cells only cultured in cell culture medium (Figure 7A, control) and also in cells exposed to hydroxyl-terminated dendrimers and to partially functionalized bis-MPA-based dendrimers (results not shown), which is in agreement with the previous cell viability experiments. When DOX is present, however, it is clear that they lose their normal shape, becoming more rounded and starting to detach from the bottom of the wells producing cell debris, thus suggesting that, probably, underwent apoptosis. After the 48 h incubation period, the cell nuclei were stained with a fluorescent probe (DAPI) and fluorescence images were captured. Because DOX is a fluorescent molecule, its cellular localization can be observed by fluorescence microscopy too. The images captured under the fluorescence microscope are in agreement with the trend in cytotoxicity observed in the previous metabolic activity assays for the CAL-72 cells. Bringing together the cell morphological results and the quantitative metabolic activity results, it is possible to say that bis-MPA-based dendrimers are promising vehicles for DOX delivery into cancer cells.

CONCLUSIONS

The objective of this work was to evaluate the in vitro behavior of bis-MPA-based dendrimers as DOX delivery carriers. When not loaded with the drug and independently of containing hydroxyl groups at the surface or being partially surface functionalized with amines, these dendrimers did not affect the viability of the cell types used in these studies. As expected, by controlling the number of amine groups at the dendrimer's periphery, the dendrimer's cytotoxicity was avoided. However, when loaded with the drug, bis-MPA-based dendrimers were able to transport it to the interior of the cells and exert cytotoxic effects. The capacity to modulate their drug-loading capacity and drug delivery profile by using different dendrimer's generation and dendrimer's terminal groups was shown. Generation 4 bis-MPA-based dendrimers may be particularly interesting as DOX delivery vehicles because they present high LC values and a sustained drug delivery behavior (drug release is slower for hydroxyl-terminated dendrimers than for amine-terminated ones). When compared with PAMAM dendrimers, bis-MPA-based dendrimers present higher DOX-loading capability and the known advantage of being biodegradable. Moreover, computational studies provided clues as to the nature of DOX interaction with bis-MPA-based dendrimers. Overall, this work suggests that the bis-MPA-based dendrimer family can be quite interesting for nanomedicine applications, namely for drug delivery purposes.

ASSOCIATED CONTENT

Supporting Information

The Supporting Information is available free of charge at https://pubs.acs.org/doi/10.1021/acs.biomac.1c00455.

NMR spectra; schematic representation of the bis-MPA-based dendrimers; drug release profile in DPBS at different pH values; And further details regarding the DOX interaction with dendrimers by MD studies (PDF)

AUTHOR INFORMATION

Corresponding Author

Helena Tomás − *CQM-Centro de Química da Madeira, MMRG, Universidade da Madeira, 9020-105 Funchal, Portugal;* orcid.org/0000-0002-7856-2041; Phone: +351291705110; Email: lenat@staff.uma.pt

Authors

Mara Gonçalves − *CQM-Centro de Química da Madeira, MMRG, Universidade da Madeira, 9020-105 Funchal, Portugal;* orcid.org/0000-0002-0332-3548

Visvaldas Kairys − *Department of Bioinformatics, Institute of Biotechnology, Life Sciences Center, Vilnius University, LT-10257 Vilnius, Lithuania;* orcid.org/0000-0002-5427-0175

João Rodrigues − *CQM-Centro de Química da Madeira, MMRG, Universidade da Madeira, 9020-105 Funchal, Portugal;* orcid.org/0000-0003-4552-1953

Complete contact information is available at: https://pubs.acs.org/10.1021/acs.biomac.1c00455

Author Contributions

The manuscript was written through the contributions of all authors. All authors have given approval to the final version of the manuscript. The authors declare no competing financial interest.

Notes

The authors declare no competing financial interest.

■ ACKNOWLEDGMENTS

The Fundação para a Ciência e Tecnologia (FCT) is acknowledged for the Ph.D. scholarship of M.G. (SFRH/BD/88721/2012) and CQM's Base Fund UIDB/00674/2020 and Programmatic Fund UIDP/00674/2020 (Portuguese Government Funds). ARDITI-Agência Regional para o Desenvolvimento da Investigação Tecnologia e Inovação and Madeira 14-20 Program are also acknowledged for project M1420-01-0145-FEDER-000005-Centro de Química da Madeira-CQM$^+$ and the postdoc grant of M.G. (ARDITI-CQM/2018/007-PDG).

■ ABBREVIATIONS

AA, antibiotic/antimycotic; bis-MPA, 2,2-bis(hydroxymethyl)-propionic acid; BOC-Gly-OH, *N*-(*tert*-butoxycarbonyl) glycine; DAPI, 4′,6-diamidino-2-phenylindole; DCC, *N*,*N*′-dicyclohexylcarbodiimide; DCM, dichloromethane; DMAP, 4-(dimethylamino)pyridine; DMF, dimethylformamide; DOX, doxorubicin; DOX·HCl, doxorubicin hydrochloride salt; DPBS, Dulbecco's phosphate-buffered saline solution; DPTS, 4-(dimethylamino) pyridinium 4-toluene sulfonate; EtOAc, ethyl acetate; FBS, fetal bovine serum; Gx, generation number; HCl, hydrochloric acid; LC, loading capacity; LE, loading efficiency; MD, molecular dynamics; PAMAM, poly(amidoamine); PEG, polyethylene glycol; PME, particle mesh Ewald; PTSA, *p*-toluenesulfonic acid monohydrate; RT, room temperature; TEA, triethylamine; THF, tetrahydrofuran

■ REFERENCES

(1) Chen, G.; Roy, I.; Yang, C.; Prasad, P. N. Nanochemistry and Nanomedicine for Nanoparticle-Based Diagnostics and Therapy. *Chem. Rev.* **2016**, *116*, 2826−2885.

(2) Shi, J.; Kantoff, P. W.; Wooster, R.; Farokhzad, O. C. Cancer Nanomedicine: Progress, Challenges and Opportunities. *Nat. Rev. Cancer* **2017**, *17*, 20−37.

(3) Karabasz, A.; Bzowska, M.; Szczepanowicz, K. Biomedical Applications of Multifunctional Polymeric Nanocarriers: A Review of Current Literature. *Int. J. Nanomed.* **2020**, *15*, 8673−8696.

(4) Mignani, S.; Rodrigues, J.; Tomas, H.; Zablocka, M.; Shi, X.; Caminade, A.-M.; Majoral, J.-P. Dendrimers in Combination with Natural Products and Analogues as Anti-Cancer Agents. *Chem. Soc. Rev.* **2018**, *47*, 514−532.

(5) Santos, A.; Veiga, F.; Figueiras, A. Dendrimers as Pharmaceutical Excipients: Synthesis, Properties, Toxicity and Biomedical Applications. *Materials* **2020**, *13*, 65−95.

(6) Tomalia, D. A.; Baker, H.; Dewald, J.; Hall, M.; Kallos, G.; Martin, S.; Roeck, J.; Ryder, J.; Smith, P. A New Class of Polymers: Starburst-Dendritic Macromolecules. *Polym. J.* **1985**, *17*, 117−132.

(7) Gonçalves, M.; Maciel, D.; Capelo, D.; Xiao, S.; Sun, W.; Shi, X.; Rodrigues, J.; Tomás, H.; Li, Y. Dendrimer-Assisted Formation of Fluorescent Nanogels for Drug Delivery and Intracellular Imaging. *Biomacromolecules* **2014**, *15*, 492−499.

(8) Liao, H.; Liu, H.; Li, Y.; Zhang, M.; Tomás, H.; Shen, M.; Shi, X. Antitumor Efficacy of Doxorubicin Encapsulated within PEGylated Poly(Amidoamine) Dendrimers. *J. Appl. Polym. Sci.* **2014**, *131*, 40358−40368.

(9) Yellepeddi, V. K.; Kumar, A.; Maher, D. M.; Chauhan, S. C.; Vangara, K. K.; Palakurthi, S. Biotinylated PAMAM Dendrimers for Intracellular Delivery of Cisplatin to Ovarian Cancer: Role of SMVT. *Anticancer Res.* **2011**, *31*, 897−906.

(10) Thanh, V. M.; Nguyen, T. H.; Tran, T. V.; Ngoc, U.-T. P.; Ho, M. N.; Nguyen, T. T.; Chau, Y. N. T.; Le, V. T.; Tran, N. Q.; Nguyen, C. K.; et al. Low Systemic Toxicity Nanocarriers Fabricated from Heparin-MPEG and PAMAM Dendrimers for Controlled Drug Release. *Mater. Sci. Eng., C* **2018**, *82*, 291−298.

(11) Vu, M. T.; Bach, L. G.; Nguyen, D. C.; Ho, M. N.; Nguyen, N. H.; Tran, N. Q.; Nguyen, D. H.; Nguyen, C. K.; Hoang Thi, T. T. Modified Carboxyl-Terminated PAMAM Dendrimers as Great Cytocompatible Nano-Based Drug Delivery System. *Int. J. Mol. Sci.* **2019**, *20*, 2016.

(12) Duncan, R.; Izzo, L. Dendrimer Biocompatibility and Toxicity. *Adv. Drug Delivery Rev.* **2005**, *57*, 2215−2237.

(13) Wolinsky, J.; Grinstaff, M. Therapeutic and diagnostic applications of dendrimers for cancer treatment☆. *Adv. Drug Delivery Rev.* **2008**, *60*, 1037−1055.

(14) Wu, L.-P.; Ficker, M.; Christensen, J. B.; Trohopoulos, P. N.; Moghimi, S. M. Dendrimers in Medicine: Therapeutic Concepts and Pharmaceutical Challenges. *Bioconjugate Chem.* **2015**, *26*, 1198−1211.

(15) Luong, D.; Kesharwani, P.; Deshmukh, R.; Mohd Amin, M. C. I.; Gupta, U.; Greish, K.; Iyer, A. K. PEGylated PAMAM Dendrimers: Enhancing Efficacy and Mitigating Toxicity for Effective Anticancer Drug and Gene Delivery. *Acta Biomater.* **2016**, *43*, 14−29.

(16) Abedi-Gaballu, F.; Dehghan, G.; Ghaffari, M.; Yekta, R.; Abbaspour-Ravasjani, S.; Baradaran, B.; Ezzati Nazhad Dolatabadi, J.; Hamblin, M. R. PAMAM Dendrimers as Efficient Drug and Gene Delivery Nanosystems for Cancer Therapy. *Appl. Mater. Today* **2018**, *12*, 177−190.

(17) Fox, L. J.; Richardson, R. M.; Briscoe, W. H. PAMAM Dendrimer - Cell Membrane Interactions. *Adv. Colloid Interface Sci.* **2018**, *257*, 1−18.

(18) Mignani, S.; Rodrigues, J.; Roy, R.; Shi, X.; Ceña, V.; El Kazzouli, S.; Majoral, J.-P. Exploration of Biomedical Dendrimer Space Based on In-Vitro Physicochemical Parameters: Key Factor Analysis (Part 1). *Drug Discovery Today* **2019**, *24*, 1176−1183.

(19) Ihre, H.; Hult, A.; Söderlind, E. Synthesis, Characterization, and 1H NMR Self-Diffusion Studies of Dendritic Aliphatic Polyesters Based on 2,2-Bis(Hydroxymethyl)Propionic Acid and 1,1,1-Tris-(Hydroxyphenyl)Ethane. *J. Am. Chem. Soc.* **1996**, *118*, 6388−6395.

(20) Carlmark, A.; Malmström, E.; Malkoch, M. Dendritic Architectures Based on Bis-MPA: Functional Polymeric Scaffolds for Application-Driven Research. *Chem. Soc. Rev.* **2013**, *42*, 5858−5879.

(21) Twibanire, J. d. A.; Grindley, T. B. Polyester Dendrimers: Smart Carriers for Drug Delivery. *Polymers* **2014**, *6*, 179−213.

(22) Zeng, X.; Zhang, Y.; Nyström, A. M. Endocytic Uptake and Intracellular Trafficking of Bis-MPA-Based Hyperbranched Copolymer Micelles in Breast Cancer Cells. *Biomacromolecules* **2012**, *13*, 3814−3822.

(23) Movellan, J.; Urbán, P.; Moles, E.; de la Fuente, J. M.; Sierra, T.; Serrano, J. L.; Fernàndez-Busquets, X. Amphiphilic Dendritic Derivatives as Nanocarriers for the Targeted Delivery of Antimalarial Drugs. *Biomaterials* **2014**, *35*, 7940−7950.

(24) Movellan, J.; González-Pastor, R.; Martín-Duque, P.; Sierra, T.; De La Fuente, J. M.; Serrano, J. L. New Ionic Bis-MPA and PAMAM Dendrimers: A Study of Their Biocompatibility and DNA-Complexation. *Macromol. Biosci.* **2015**, *15*, 657−667.

(25) Lancelot, A.; González-Pastor, R.; Concellón, A.; Sierra, T.; Martín-Duque, P.; Serrano, J. L. DNA Transfection to Mesenchymal Stem Cells Using a Novel Type of Pseudodendrimer Based on 2,2-Bis(Hydroxymethyl)Propionic Acid. *Bioconjugate Chem.* **2017**, *28*, 1135−1150.
(26) Martí Coma-Cros, E.; Lancelot, A.; San Anselmo, M.; Neves Borgheti-Cardoso, L.; Valle-Delgado, J. J.; Serrano, J. L.; Fernàndez-Busquets, X.; Sierra, T. Micelle Carriers Based on Dendritic Macromolecules Containing Bis-MPA and Glycine for Antimalarial Drug Delivery. *Biomater. Sci.* **2019**, *7*, 1661−1674.
(27) Feliu, N.; Walter, M. V.; Montañez, M. I.; Kunzmann, A.; Hult, A.; Nyström, A.; Malkoch, M.; Fadeel, B. Stability and Biocompatibility of a Library of Polyester Dendrimers in Comparison to Polyamidoamine Dendrimers. *Biomaterials* **2012**, *33*, 1970−1981.
(28) Stenström, P.; Manzanares, D.; Zhang, Y.; Ceña, V.; Malkoch, M. Evaluation of Amino-Functional Polyester Dendrimers Based on Bis-MPA as Nonviral Vectors for SiRNA Delivery. *Molecules* **2018**, *23*, 2028.
(29) Stenström, P.; Hjorth, E.; Zhang, Y.; Andrén, O. C. J.; Guette-Marquet, S.; Schultzberg, M.; Malkoch, M. Synthesis and in Vitro Evaluation of Monodisperse Amino-Functional Polyester Dendrimers with Rapid Degradability and Antibacterial Properties. *Biomacromolecules* **2017**, *18*, 4323−4330.
(30) Tacar, O.; Sriamornsak, P.; Dass, C. R. Doxorubicin: An Update on Anticancer Molecular Action, Toxicity and Novel Drug Delivery Systems. *J. Pharm. Pharmacol.* **2012**, *65*, 157−170.
(31) Gonçalves, M.; Mignani, S.; Rodrigues, J.; Tomás, H. A Glance over Doxorubicin Based-Nanotherapeutics: From Proof-of-Concept Studies to Solutions in the Market. *J. Controlled Release* **2020**, *317*, 347−374.
(32) Barenholz, Y.; Gabizon, A. Liposome/Doxorubicin Compositon and Method. U.S. Patent 4,898,735 A, 1990.
(33) James, N. D.; Coker, R. J.; Tomlinson, D.; Harris, J. R. W.; Gompels, M.; Pinching, A. J.; Stewart, J. S. W. Liposomal doxorubicin (Doxil): An effective new treatment for Kaposi's sarcoma in AIDS. *Clin. Oncol.* **1994**, *6*, 294−296.
(34) Batist, G.; Barton, J.; Chaikin, P.; Swenson, C.; Welles, L. Myocet (Liposome-Encapsulated Doxorubicin Citrate): A New Approach in Breast Cancer Therapy. *Expert Opin. Pharmacother.* **2002**, *3*, 1739−1751.
(35) Reagan, M. R.; Kaplan, D. L. Concise Review: Mesenchymal Stem Cell Tumor-Homing: Detection Methods in Disease Model Systems. *Stem Cells* **2011**, *29*, 920−927.
(36) Chang, A.; Schwertschkow, A.; Nolta, J.; Wu, J. Involvement of Mesenchymal Stem Cells in Cancer Progression and Metastases. *Curr. Cancer Drug Targets* **2015**, *15*, 88−98.
(37) Rhee, K.-J.; Lee, J.; Eom, Y. Mesenchymal Stem Cell-Mediated Effects of Tumor Support or Suppression. *Int. J. Mol. Sci.* **2015**, *16*, 30015−30033.
(38) Khanal, B. P.; Zubarev, E. R. Rings of Nanorods. *Angew. Chem., Int. Ed.* **2007**, *46*, 2195−2198.
(39) Wu, H.; Zhu, H.; Zhuang, J.; Yang, S.; Liu, C.; Cao, Y. C. Water-Soluble Nanocrystals through Dual-Interaction Ligands. *Angew. Chem., Int. Ed.* **2008**, *47*, 3730−3734.
(40) Deng, H.; Zhao, X.; Liu, J.; Zhang, J.; Deng, L.; Liu, J.; Dong, A. Synergistic Dual-pH Responsive Copolymer Micelles for pH-Dependent Drug Release. *Nanoscale* **2016**, *8*, 1437−1450.
(41) Pettersen, E. F.; Goddard, T. D.; Huang, C. C.; Couch, G. S.; Greenblatt, D. M.; Meng, E. C.; Ferrin, T. E. UCSF Chimera?A visualization system for exploratory research and analysis. *J. Comput. Chem.* **2004**, *25*, 1605−1612.
(42) Hanwell, M. D.; Curtis, D. E.; Lonie, D. C.; Vandermeersch, T.; Zurek, E.; Hutchison, G. R. Avogadro: An Advanced Semantic Chemical Editor, Visualization, and Analysis Platform. *J. Cheminf.* **2012**, *4*, 1−17.
(43) Halgren, T. A. MMFF VI. MMFF94s Option for Energy Minimization Studies. *J. Comput. Chem.* **1999**, *20*, 720−729.
(44) Maiti, P. K.; Çağın, T.; Wang, G.; Goddard, W. A. Structure of PAMAM Dendrimers: Generations 1 through 11. *Macromolecules* **2004**, *37*, 6236−6254.
(45) Howerton, S. B.; Nagpal, A.; Dean Williams, L. Surprising Roles of Electrostatic Interactions in DNA-Ligand Complexes. *Biopolymers* **2003**, *69*, 87−99.
(46) Jorgensen, W. L.; Chandrasekhar, J.; Madura, J. D.; Impey, R. W.; Klein, M. L. Comparison of Simple Potential Functions for Simulating Liquid Water. *J. Chem. Phys.* **1983**, *79*, 926−935.
(47) Berendsen, H. J. C.; van der Spoel, D.; van Drunen, R. GROMACS: A Message-Passing Parallel Molecular Dynamics Implementation. *Comput. Phys. Commun.* **1995**, *91*, 43−56.
(48) Jorgensen, W. L.; Maxwell, D. S.; Tirado-Rives, J. Development and Testing of the OPLS All-Atom Force Field on Conformational Energetics and Properties of Organic Liquids. *J. Am. Chem. Soc.* **1996**, *118*, 11225−11236.
(49) He, X.; Alves, C. S.; Oliveira, N.; Rodrigues, J.; Zhu, J.; Bányai, I.; Tomás, H.; Shi, X. RGD Peptide-Modified Multifunctional Dendrimer Platform for Drug Encapsulation and Targeted Inhibition of Cancer Cells. *Colloids Surf., B* **2015**, *125*, 82−89.
(50) Khopade, A. J.; Caruso, F. Stepwise Self-Assembled Poly-(Amidoamine) Dendrimer and Poly(Styrenesulfonate) Microcapsules as Sustained Delivery Vehicles. *Biomacromolecules* **2002**, *3*, 1154−1162.
(51) Wang, Y.; Cao, X.; Guo, R.; Shen, M.; Zhang, M.; Zhu, M.; Shi, X. Targeted Delivery of Doxorubicin into Cancer Cells Using a Folic Acid-Dendrimer Conjugate. *Polym. Chem.* **2011**, *2*, 1754−1760.
(52) Song, C.; Xiao, Y.; Ouyang, Z.; Shen, M.; Shi, X. Efficient Co-Delivery of MicroRNA 21 Inhibitor and Doxorubicin to Cancer Cells Using Core-Shell Tecto Dendrimers Formed via Supramolecular Host-Guest Assembly. *J. Mater. Chem. B* **2020**, *8*, 2768−2774.
(53) Zeng, X.; Zhang, Y.; Wu, Z.; Lundberg, P.; Malkoch, M.; Nyström, A. M. Hyperbranched Copolymer Micelles as Delivery Vehicles of Doxorubicin in Breast Cancer Cells. *J. Polym. Sci., Part A: Polym. Chem.* **2012**, *50*, 280−288.
(54) Arcon, J. P.; Defelipe, L. A.; Modenutti, C. P.; López, E. D.; Alvarez-Garcia, D.; Barril, X.; Turjanski, A. G.; Martí, M. A. Molecular Dynamics in Mixed Solvents Reveals Protein-Ligand Interactions, Improves Docking, and Allows Accurate Binding Free Energy Predictions. *J. Chem. Inf. Model.* **2017**, *57*, 846−863.
(55) Graham, S. E.; Leja, N.; Carlson, H. A. MixMD Probeview: Robust Binding Site Prediction from Cosolvent Simulations. *J. Chem. Inf. Model.* **2018**, *58*, 1426−1433.
(56) Rizzo, V.; Sacchi, N.; Menozzi, M. Kinetic Studies of Anthracycline-DNA Interaction by Fluorescence Stopped Flow Confirm a Complex Association Mechanism. *Biochemistry* **1989**, *28*, 274−282.
(57) Tasca, E.; Alba, J.; Galantini, L.; D'Abramo, M.; Giuliani, A. M.; Amadei, A.; Palazzo, G.; Giustini, M. The Self-Association Equilibria of Doxorubicin at High Concentration and Ionic Strength Characterized by Fluorescence Spectroscopy and Molecular Dynamics Simulations. *Colloids Surf., A* **2019**, *577*, 517−522.
(58) Neel, A. J.; Hilton, M. J.; Sigman, M. S.; Toste, F. D. Exploiting non-covalent π interactions for catalyst design. *Nature* **2017**, *543*, 637−646.
(59) Agrawal, P.; Barthwal, S. K.; Barthwal, R. Studies on Self-Aggregation of Anthracycline Drugs by Restrained Molecular Dynamics Approach Using Nuclear Magnetic Resonance Spectroscopy Supported by Absorption, Fluorescence, Diffusion Ordered Spectroscopy and Mass Spectrometry. *Eur. J. Med. Chem.* **2009**, *44*, 1437−1451.
(60) Roberts, J. C.; Bhalgat, M. K.; Zera, R. T. Preliminary biological evaluation of polyamidoamine (PAMAM) StarburstTM dendrimers. *J. Biomed. Mater. Res.* **1996**, *30*, 53−65.
(61) Malik, N.; Wiwattanapatapee, R.; Klopsch, R.; Lorenz, K.; Frey, H.; Weener, J. W.; Meijer, E. W.; Paulus, W.; Duncan, R. Dendrimers: *J. Controlled Release* **2000**, *65*, 133−148.
(62) Kolhatkar, R. B.; Kitchens, K. M.; Swaan, P. W.; Ghandehari, H. Surface Acetylation of Polyamidoamine (PAMAM) Dendrimers

Decreases Cytotoxicity While Maintaining Membrane Permeability. *Bioconjugate Chem.* **2007**, *18*, 2054−2060.
(63) King Heiden, T. C.; Dengler, E.; Kao, W. J.; Heideman, W.; Peterson, R. E. Developmental Toxicity of Low Generation PAMAM Dendrimers in Zebrafish. *Toxicol. Appl. Pharmacol.* **2007**, *225*, 70−79.
(64) Goncalves, M.; Castro, R.; Rodrigues, J.; Tomás, H. The Effect of PAMAM Dendrimers on Mesenchymal Stem Cell Viability and Differentiation. *Curr. Med. Chem.* **2012**, *19*, 4969−4975.
(65) Bodewein, L.; Schmelter, F.; Di Fiore, S.; Hollert, H.; Fischer, R.; Fenske, M. Differences in Toxicity of Anionic and Cationic PAMAM and PPI Dendrimers in Zebrafish Embryos and Cancer Cell Lines. *Toxicol. Appl. Pharmacol.* **2016**, *305*, 83−92.

https://doi.org/10.1021/acs.biomac.1c00455
Biomacromolecules 2022, 23, 20−33